Submitted to
HEP2005 International Europhysics Conference on High Energy Physics, 21-27 July 2005, Lisboa
Abstract: **635**
Session: **Physics beyond the Standard Model**
www-h1.desy.de/h1/www/publications/conf/conf_list.html

Multi–lepton events at HERA and a General Search for New Phenomena at Large Transverse Momentum

H1 Collaboration

Abstract

Search for multi–lepton events is performed on a data sample collected in $e^{\pm}p$ collisions with the H1 detector at HERA in the period 1994–2005. This data sample corresponds to an integrated luminosity of 209 pb^{-1}, which includes 45 pb^{-1} of $e^{+}p$ data taken in 2004 and 40 pb^{-1} of $e^{-}p$ data taken in 2005. Results on a general search for new phenomena using the 2004 data only are also presented.

1 Multi-lepton Analysis

Multi–lepton (electron or muon) production is measured at high transverse momentum using the full HERA data sample. In addition to an update of the published HERA I multi-electron and multi-muon analyses, new topologies with high P_T electrons and muons are investigated here for the first time. Yields of di-lepton and tri-lepton events are measured and a general good agreement is found with the Standard Model predictions. However, combining all channels, four events are observed with a scalar sum of lepton transverse momenta greater than 100 GeV, compared to a Standard Model expectation of 0.61 ± 0.11.

1.1 Introduction

Within the Standard Model (SM) the production of multi-lepton events in ep collisions mainly proceeds via photon-photon interactions [1]. Precise cross-section measurements of both electron (e) and muon (μ) pair production at high transverse momentum (P_T) have already been performed by the H1 collaboration [2, 3]. At large di-electron masses, an excess of events is observed in both the di-electron and tri-electron samples [2].

The present analysis extends our previous measurements to the eμ and e$\mu\mu$ topologies and to a higher luminosity, combining new HERA II data taken in 2003–2004 ($\mathcal{L} = 45$ pb^{-1}) and 2005 ($\mathcal{L} = 40$ pb^{-1}) with the previous HERA I data sample from 1994–2000 ($\mathcal{L} = 118$ pb^{-1}).

1.2 Standard Model Processes and their Simulation

Multi–lepton events are generated with the GRAPE [4] program, which includes all electroweak matrix elements at tree level. Multi-lepton production via $\gamma\gamma$, γZ, ZZ collisions, internal photon conversion and the decay of virtual or real Z bosons is considered. Initial and final state QED radiation is included. The complete hadronic final state is simulated via interfaces to PYTHIA and SOPHIA [5] for the inelastic and quasi-elastic regimes, respectively. Consequently, GRAPE predicts $ep \to \mu\mu X$ and $ep \to eeX$, as well as $ep \to e\mu\mu X$ and $ep \to eeeX$ if the scattered electron is detected. The $ep \to \tau\tau X$ process is also simulated with GRAPE and its contribution was found to be negligible.

The dominant background contributions arise from neutral current deep-inelastic scattering (DIS) events ($ep \to eX$) [2]. QED Compton scattering $ep \to e\gamma X$ can also contribute. The DIS and elastic Compton processes are simulated using the RAPGAP [6] (for HERA I) or DJANGO [7] (HERA II) and WABGEN [8] generators, respectively.

All generated events are passed through the full GEANT [9] based simulation of the H1 apparatus, which takes into account the running conditions of the different data taking periods.

1.3 Multi-lepton Event Selection

The electron identification procedure follows the criteria described in [2]. Electron candidates with energies above 5 GeV are identified in the liquid argon and backward calorimeters, in the range $5^\circ < \theta < 175^\circ$. Electron candidates are required to be isolated by demanding that they are separated from other leptons or jets by at least 0.5 units in the pseudorapidity-azimuth ($\eta - \phi$) plane. In addition, the total hadronic energy within 0.75 units in $\eta - \phi$ of the electron direction is required to be below 2.5 % of the electron energy. In the region of angular overlap between the liquid argon calorimeter and the central drift chambers ($20^\circ < \theta < 150^\circ$), the calorimetric electron identification is complemented by tracking conditions. In this region it is required that a high quality track geometrically matches the electromagnetic cluster within a distance of closest approach to the cluster centre-of-gravity of 12 cm. No other good track is allowed within 0.5 units in $\eta - \phi$ around the electron direction. In the central region ($20^\circ < \theta < 150^\circ$) the distance between the first measured point in the central drift chambers and the beam axis is required to be below 30 cm in order to reject photons that convert late in the central tracker material. In addition, in this central region, the transverse momentum measured from the associated track $P_T^{e_{tk}}$ is required to match the calorimetric measurement P_T^e with $1/P_T^{e_{tk}} - 1/P_T^e < 0.02$ GeV^{-1}. This criteria is relaxed to 0.04 for the new HERA II data since a final calibration and alignment have not been performed. Due to the higher material density in the forward region ($5^\circ < \theta < 20^\circ$) the electrons are more likely to shower and therefore no track conditions are required. The same applies in the backward region ($150^\circ < \theta < 175^\circ$). The electron energy threshold is raised to 10 GeV in the forward region.

Muon candidates are identified with a $P_T > 2$ GeV in the range $20^\circ < \theta < 160^\circ$, with a similar procedure to that described in [3]. The muon identification is based on a track in the forward muon system or the inner tracking systems associated with a track segment or an energy deposit in the instrumented iron [10]. The momentum of the muons detected in the forward muon detector is measured from the curvature in a toroidal magnetic field. The muon momentum is measured in the central region from the track curvature in the solenoidal magnetic field. A muon candidate should have no more than 5 GeV deposited in the LAr calorimeter in a cylinder of radius 25 cm and 50 cm in the electromagnetic and hadronic sections of the LAr calorimeter, respectively, centred on the muon track direction. In di-muon events, the requirement of an opening angle between the two muons smaller than 160° discards cosmic rays background. Beam halo events are rejected by requiring that the muons originate from the event vertex. Finally, misidentified hadrons are strongly suppressed by requiring that the muon candidate is separated from the closest jet and from any good quality track by 1 unit in the $\eta - \phi$ plane. Muon canditates are also required to be isolated from other leptons by at least 0.5 units in the $\eta - \phi$ plane.

The final multi-lepton selection requires that there be at least two central ($20^\circ < \theta < 150^\circ$) lepton (electron or muon) candidates, of which one must have $P_T^l > 10$ GeV and the other $P_T^l > 5$ GeV. Additional lepton candidates are identified in the detector according to the above criteria without any additional explicit P_T or angular requirements. The lepton candidates are ordered according to decreasing P_T, $P_T^{l_i} > P_T^{l_{i+1}}$. The selected events are classified as belonging to the two lepton sample if only two central leptons are identified, and to the three lepton sample if exactly one additional lepton candidate is identified. According to the flavours of the identified leptons, these samples are further classified into ee, $\mu\mu$, eμ, eee and e$\mu\mu$.

1.4 Results

The event yields observed in all channels are summarised in table 1. The observed event yields are in good agreement with SM expectations, which are dominated by pair production.

The distributions of the invariant mass of the two leptons in the di-lepton event classes are presented in figure 1. The agreement with the SM prediction is good, except in the ee invariant mass distribution for $M_{12} > 100$ GeV, where the three events already described in [2] are present, compared to an expectation of 0.61 $\pm$ 0.14 (see table 2). The distribution of the invariant mass M_{12} of the two highest P_T electrons for the eee sample is shown in figure 2, as well as the invariant mass combinations of the electron with the higest P_T muon ($M_{e\mu}$) and of both muons ($M_{\mu\mu}$) in the e$\mu\mu$ sample. The event yields in the tails of invariant mass distributions ($M > 100$ GeV) of all channels are summarised in table 2. The three "ee" events with $M_{12} > 100$ GeV are observed in HERA I data and are discussed in [2], as well as the three "eee" with $M_{12} > 100$ GeV. Two e$\mu\mu$ events are observed in the new HERA II data, of which one has a high muon-muon and the other a high electron-muon invariant mass. The e$\mu\mu$ event with the high $M_{e\mu}$ invariant mass is shown in figure 3.

The distributions of the scalar sum of P_T of all identified leptons for the di and tri–lepton samples and the combination of both is shown in figure 4. For $\sum P_T > 100$ GeV 4 events are observed in all channels combined while 0.81 $\pm$ 0.14 are expected. These four data events correspond to the three ee events observed in HERA I data [2] and one new e$\mu\mu$ event observed in HERA II data.

The separation of the total HERA data sample between events taken in collisions with a positron or electron beam is also presented in figure 4 and in table 2. All high invariant masses and $\sum P_T$ events have been recorded in e^+p collisions and none is shonw in e^-p data.

1.5 Summary

The production of multi-leptons (electrons and muons) at high transverse momenta in ep scattering has been studied. The measurement extends previous analyses [2, 3] by including the HERA II data recorded in e^+p and $e-p$ collisions and corresponding to integrated luminosities luminosity of 45 pb$^-1$ and 40 pb$^-1$, respectively. The event yields in the di-lepton (ee, $\mu\mu$ and eμ) and tri-lepton (eee and e$\mu\mu$) sub-samples are in good agreement with the SM predictions. The distribution of the scalar sum of transverse momenta of the leptons is studied for the combination of all di- and tri-lepton sub-samples. For $\sum P_T > 100$ GeV 4 events are observed and 0.81 $\pm$ 0.14 are expected.

References

[1] J. A. M. Vermaseren, Nucl. Phys. B **229** (1983) 347.

[2] A. Aktas *et al.* [H1 Collaboration], Eur. Phys. J. C **31** (2003) 17 [hep-ex/0307015].

[3] A. Aktas *et al.* [H1 Collaboration], Phys. Lett. B **583** (2004) 28 [hep-ex/0311015].

[4] T. Abe, Comput. Phys. Commun. **136** (2001) 126 [hep-ph/0012029].

[5] A. Mucke, R. Engel, J. P. Rachen, R. J. Protheroe and T. Stanev, Comput. Phys. Commun. **124** (2000) 290 [astro-ph/9903478].

[6] H. Jung, Comput. Phys. Commun. **86** (1995) 147.

[7] G. A. Schuler and H. Spiesberger, "Django: The Interface for The Event Generators Heracles and Lepto."

[8] C. Berger and P. Kandel, Prepared for Workshop on Monte Carlo Generators for HERA Physics Hamburg, Germany, 27-30 Apr 1998.

[9] R. Brun, F. Bruyant, M. Maire, A. C. McPherson and P. Zanarini, CERN-DD/EE/84-1.

[10] V. Andreev *et al.* [H1 Collaboration], Phys. Lett. B **561** (2003) 241 [hep-ex/0301030].

H1 Preliminary 209 pb^{-1} (1994-2005)

Selection	Data	SM	Pair Production (GRAPE)	NC-DIS + Compton
ee	190	196 ± 29	163 ± 17	33 ± 20
$\mu\mu$	82	85 ± 16	85 ± 16	—
eμ	106	99 ± 13	61 ± 5	38 ± 10
eee	37	39 ± 4	39 ± 4	0.1 ± 0.1
e$\mu\mu$	50	51 ± 8	51 ± 8	—

Table 1: Observed and predicted event yields for the ee, $\mu\mu$, eμ, eee and e$\mu\mu$ event classes. The analysed data sample corresponds to an integrated luminosity of 209 pb^{-1}. The errors on the prediction include model uncertainties and experimental systematic errors added in quadrature.

H1 Preliminary 209 pb^{-1} (1994-2005)

Selection	Data	SM	Pair Production (GRAPE)	NC-DIS + Compton
e^+p collisions				
ee M_{12} >100 GeV	3	0.44 ± 0.10	0.29 ± 0.09	0.15 ± 0.04
$\mu\mu$ $M_{\mu\mu}$ >100 GeV	0	0.035 ± 0.02	0.035 ± 0.02	—
eμ $M_{e\mu}$ >100 GeV	0	0.29 ± 0.03	0.29 ± 0.03	—
eee M_{12} >100 GeV	3	0.29 ± 0.06	0.29 ± 0.06	—
e$\mu\mu$ $M_{e\mu}$ >100 GeV	1	0.04 ± 0.01	0.04 ± 0.01	—
e$\mu\mu$ $M_{\mu\mu}$ >100 GeV	1	0.015 ± 0.007	0.015 ± 0.007	—
e^-p collisions				
ee M_{12} >100 GeV	0	0.17 ± 0.04	0.10 ± 0.03	0.07 ± 0.02
$\mu\mu$ $M_{\mu\mu}$ >100 GeV	0	0.012 ± 0.01	0.012 ± 0.01	—
eμ $M_{e\mu}$ >100 GeV	0	0.11 ± 0.02	0.11 ± 0.02	—
eee M_{12} >100 GeV	0	0.1 ± 0.03	0.1 ± 0.03	—
e$\mu\mu$ $M_{e\mu}$ >100 GeV	0	0.01 ± 0.003	0.01 ± 0.003	—
e$\mu\mu$ $M_{\mu\mu}$ >100 GeV	0	0.005 ± 0.003	0.005 ± 0.003	—
All data				
ee M_{12} >100 GeV	3	0.61 ± 0.14	0.39 ± 0.12	0.22 ± 0.06
$\mu\mu$ $M_{\mu\mu}$ >100 GeV	0	0.047 ± 0.03	0.047 ± 0.03	—
eμ $M_{e\mu}$ >100 GeV	0	0.40 ± 0.04	0.40 ± 0.04	—
eee M_{12} >100 GeV	3	0.39 ± 0.07	0.39 ± 0.07	—
e$\mu\mu$ $M_{e\mu}$ >100 GeV	1	0.05 ± 0.015	0.05 ± 0.015	—
e$\mu\mu$ $M_{\mu\mu}$ >100 GeV	1	0.02 ± 0.01	0.02 ± 0.01	—

Table 2: Yields for high di-lepton masses, $M > 100$ GeV in all analysed samples. For the eee sample, the mass of the two highest P_T electrons is shown. The analysed data sample corresponds to an integrated luminosity of 209 pb^{-1}. The errors on the prediction include model uncertainties and experimental systematic errors added in quadrature.

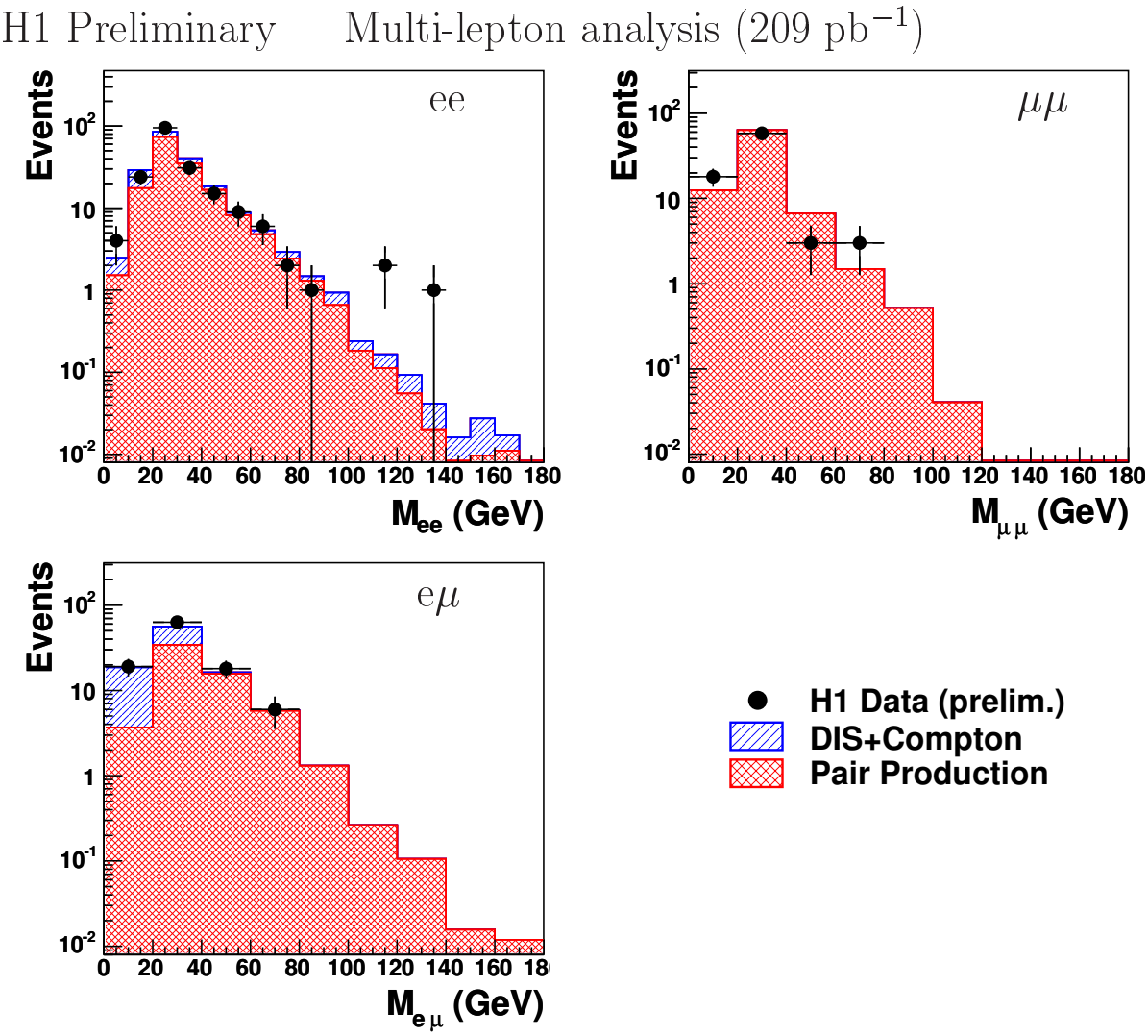

Figure 1: Distibution of the invariant mass M of the two leptons compared to expectations for events classified as ee, $\mu\mu$ and eμ. The analysed data sample corresponds to an integrated luminosity of 209 pb^{-1}.

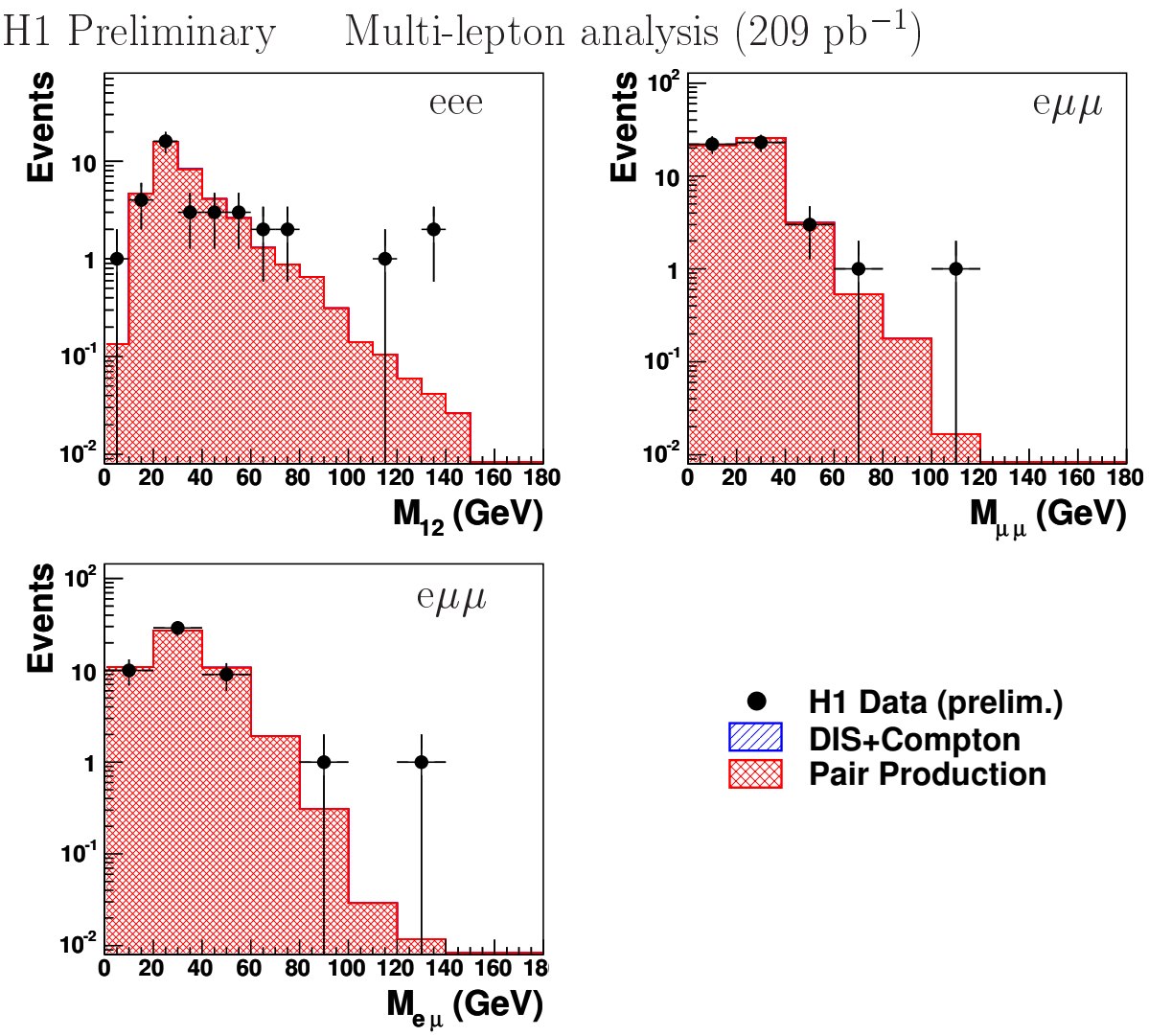

Figure 2: Distribution of the invariant mass M_{12} of the two highest P_T electrons for the eee sample (top left). For the e$\mu\mu$ sample, invariant mass combinations of the electron with the higest P_T muon ($M_{e\mu}$, bottom left) and of both muons ($M_{\mu\mu}$, top right) are presented. The analysed data sample corresponds to an integrated luminosity of 209 pb^{-1}.

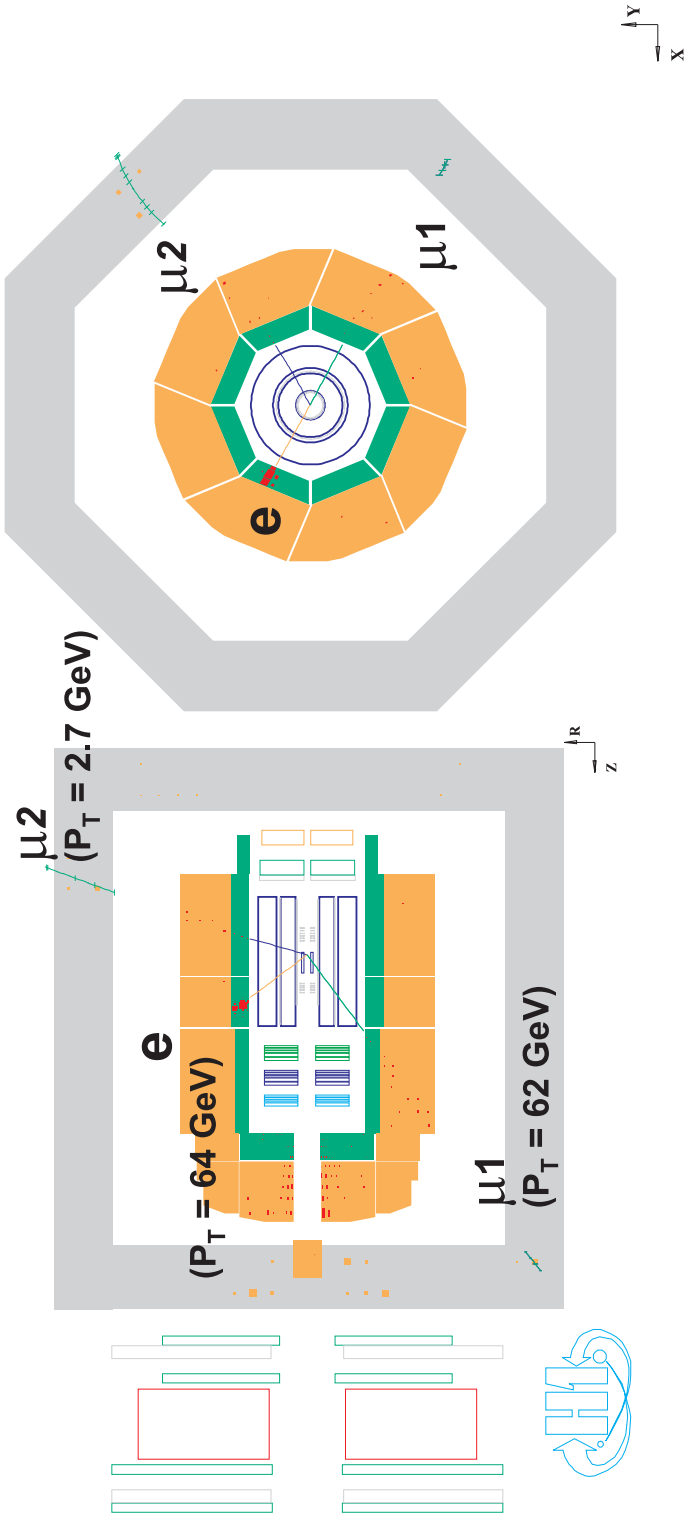

Figure 3: Display of the e$\mu\mu$ event with a scalar sum of transverse momenta of the leptons $\sum P_T > 100$ GeV, observed in the new HERA II data.

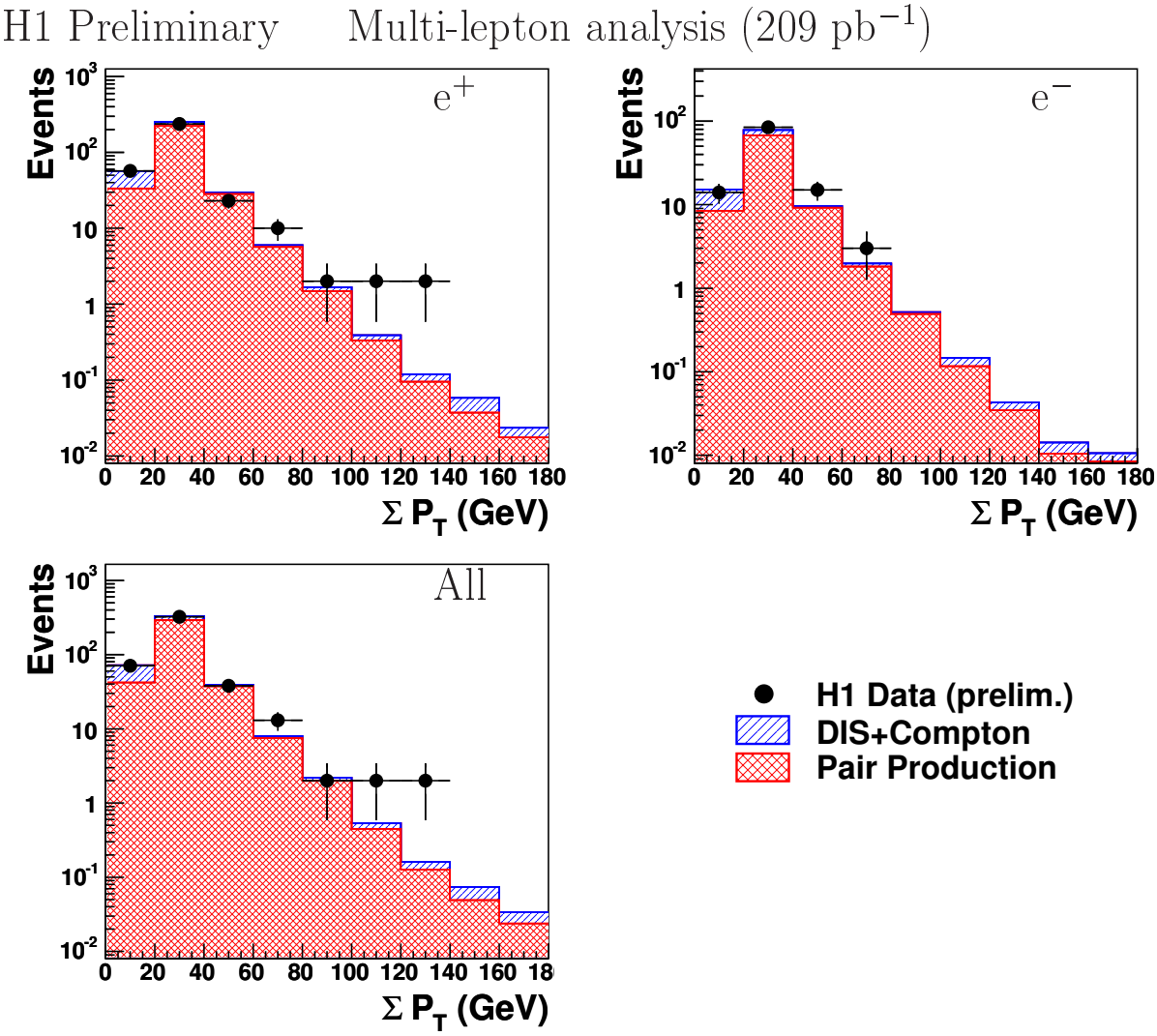

Figure 4: Distributions of the scalar sum of the transverse momenta of leptons compared to expectations for data taken in e^+p (upper left) and e^-p (upper right) collisions. The Combination of all HERA data is shown in the bottom figure. The analysed data sample corresponds to an integrated luminosity of 209 pb^{-1}.

2 General Search Analysis

2.1 Introduction

The general search for new physics involving high P_T particle production consists of a comprehensive and generic search for deviations from the SM prediction using all high P_T final state configurations involving electrons (e), muons (μ), jets (j), photons (γ) or neutrinos (ν). The analysis covers phase space regions where the SM prediction is sufficiently precise to detect anomalies and does not rely on assumptions concerning the characteristics of any SM extension. Such a model-independent approach may discover unexpected manifestations of new physics.

Results obtained with HERA I data ($\mathcal{L} = 115$ pb^{-1}) have previously been published [1]. The results from the HERA II data sample ($\mathcal{L} = 45$ pb^{-1}) are presented here.

2.2 Analysis of HERA II Data

As in the HERA I analysis, all final states containing at least two objects (e, μ, j, γ, ν) with $P_T > 20$ GeV in the polar angle range $10^\circ < \theta < 140^\circ$ are investigated. All selected events are classified into exclusive event classes according to the number and types of objects detected in the final state, for example ej, $\mu j\nu$, $jjjj$.

Figure 5 shows the yields obtained in the various event classes. Good agreement with the SM expectation is observed in all event classes, indicating the good understanding of the SM predictions for HERA and of the H1 detector in the HERA II configuration. The majority of the events observed in the dedicated multi–lepton and isolated lepton analyses are also selected in this general analysis.

References

[1] H1Colaboration, "General search for new phenomena in ep scattering at HERA" DESY 04-140, submitted to Phys.Lett. [h1p-ex 0408044]

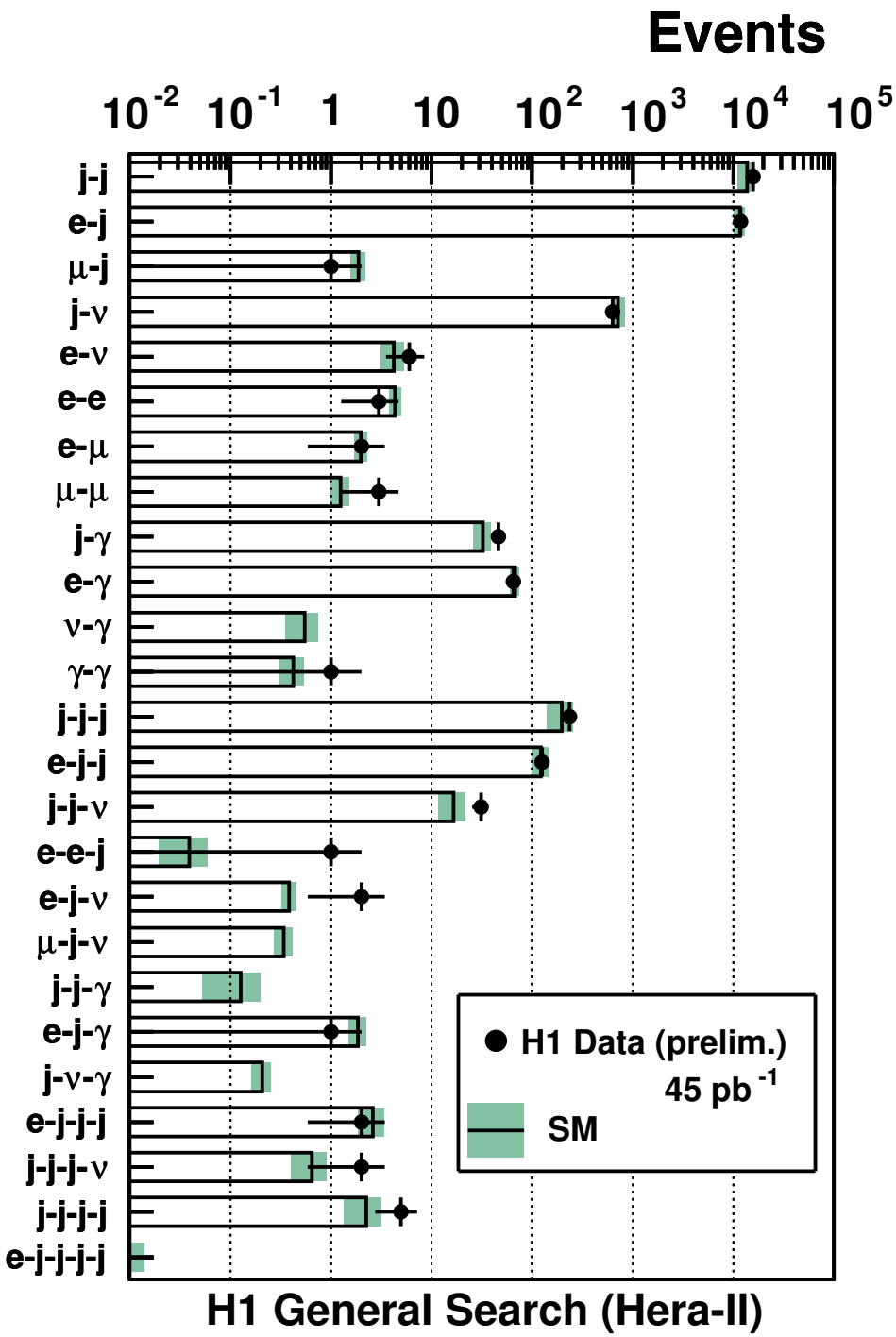

Figure 5: Results of the H1 general search using the new HERA II data (2003-2004). The analysed data sample corresponds to an integrated luminosity of 45 pb^{-1}. The errors on the prediction include model uncertainties and experimental errors added in quadrature.